Influence of defect states on the nonlinear optical properties of GaN

H. Haag and B. Hönerlage
Groupe d'Optique Nonlinéaire et d'Optoélectronique, Institut de Physique et Chimie des Matériaux de Strasbourg, UMR 7504 CNRS-ULP, 23, Rue du Loess, Boîte Postale 20CR, F-67037 Strasbourg Cedex, France

O. Briot and R. L. Aulombard
Groupe d'Étude des Semiconducteurs, URA 357 CNRS-Université de Montpellier II, Place Eugène Bataillon, F-34095 Montpellier Cedex 05, France

(Received 8 March 1999)

We study the influence of defect states (shallow donors and deep acceptors) on the carrier relaxation dynamics of gallium nitride in the picosecond regime for different excitation intensities and different lattice temperatures. Time-resolved luminescence, degenerate, and nondegenerate four-wave mixing experiments show a saturation threshold in the blue and yellow spectral region, which is found to disappear for lattice temperatures below 200 K. When analyzing all these results in the frame of a rate-equation model, we give a relaxation scenario for the carriers, the lifetimes of the population of the different states, and identify radiative and nonradiative transitions. After filling defect states by an optical excitation, the ambipolar diffusion coefficient of GaN is measured through degenerate four-wave mixing experiments. A low value of 0.16 cm^2/s at room temperature is determined, indicating that defect states still influence the diffusion. Nondegenerate four-wave mixing experiments exhibit a competition between an electronical and a thermal contribution to the nonlinear susceptibility in GaN. [S0163-1829(99)00340-9]

I. INTRODUCTION

The quest for semiconductor lasers emitting in the blue and UV spectral regions is on the point of ending with the realization of nitride compound devices.[1] Indeed, light emitting diodes and semiconductor lasers emitting in the blue spectral region are now commercially available,[2] despite the high density of native or extrinsic defects present in the layers.[3] The small influence of these defect levels on nitride devices is still not explained. They are expected to give rise to radiative and nonradiative effects, the most common of which is the emission of a broad luminescence band near 2.3 eV, the so-called ''yellow luminescence.'' This band, which is observed independently of the growth process, is generally attributed to structural defects.[4] One of the difficulties to determine the origin of these deep states is due to the fact that the corresponding levels are not observed in reflection or transmission measurements. Therefore, the origin of the yellow line was attributed either to a recombination from a deep double donor to a shallow acceptor[5] or to that of a shallow donor to a deep acceptor center.[6,7] Several pertinent results[8–11] seem, however, to support the last model, i.e., that the yellow luminescence is due to an electronic recombination between shallow donors (also responsible for the I_2 line) and a deep state located about 1 eV above the valence band. On the other hand, it is also commonly accepted that their nonradiative recombination reduces the lifetime of the carriers.[12]

In this paper, we study the influence of these states on the nonlinear optical properties of GaN in the blue and yellow spectral region. After a description of our samples and of the different experimental setups used, we present results of time-resolved luminescence, nondegenerate and degenerate four-wave mixing experiments. Our measurements are first performed at room temperature in the picosecond regime. They lead to the determination of the complete set of recombination times of the different levels present in GaN and their occupation dynamics. These studies are completed by temperature dependence measurements, in order to determine a possible origin of the observed saturation processes.

II. SAMPLES AND EXPERIMENTAL SETUP

The core of this article is based on a nonintentionally doped GaN epilayer grown by metal-organic chemical vapor deposition (MOCVD) on a (0001) sapphire substrate with a AlN prebuffer. The growth temperature is about 1250 K, the III/V molar ratio worth about 10 000 and the thickness of the layer is 1.2 μm. Since we focus throughout this work on the influence of deep levels, we study a sample that exhibits a bright yellow luminescence band, shown on Fig. 1. The ratio r between the integrated intensities of the blue and the yellow luminescence is about 50. Nevertheless, as has been shown in Ref. 13, the optical quality of the sample is good enough to show some excitonic structures in its linear luminescence spectrum at low temperature. They correspond to the D^0-X, A- and B-exciton lines, respectively.

This sample is compared with two other ones, also grown by MOCVD on a sapphire substrate with a growth temperature of about 1250 K. Their ratio r, which gives an indication of their optical quality, is found to be equal to 0.5 and 400, respectively. The sample with $r=0.5$ is thinner than the sample of reference (0.35 μm) and is grown with a III/V molar ratio equal to 10 000. The sample with $r=400$ is grown on a GaN prebuffer with a molar III/V ratio equal to 8000. The thickness of the layer is 0.8 μm.

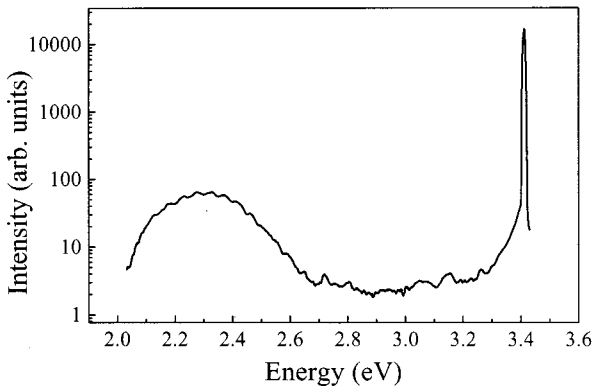

FIG. 1. Linear luminescence spectra of our GaN sample at room temperature.

Time-resolved luminescence experiments are performed by exciting the sample with the fourth harmonic of a Nd:YAG laser, emitting pulses of 25 ps duration at 4.66 eV with a repetition rate of 5 Hz. Using neutral density filters, the pulse intensity is varied up to 1 MW cm^{-2}, which is close to the destruction threshold of the sample. We select the blue or the yellow luminescence using color filters and focus the luminescence signal on the entrance slit of a Streak camera. In order to control the fluctuations induced by intensity variations of the excitation, the pump pulse intensity is discriminated and only pump pulses whose intensities lie within a window of $\pm 10\%$ around a mean value are considered when the signals are readout. In order to increase the signal to noise ratio, measurements are averaged over 300 laser shots. Then, the overall time resolution of the system is about 10 ps.

In wave-mixing experiments, carriers are generated by a band-to-band excitation with the third harmonic ($\hbar\omega_p = 3.49$ eV, $\lambda_P = 355$ nm) of the Nd:YAG laser, used as excitation beam. A light-induced grating is produced by splitting the excitation pulses into two parts of equal intensities and by focusing both at temporal coincidence onto the sample with an angle θ. By this way, we generate a transient grating with a fringe spacing $\Lambda = \lambda_P/2\sin(\theta/2)$, which goes from 2 to 14 μm by varying θ. We measure the diffracted intensity of a third pulse (probe) with a Reticon camera. This third pulse is either degenerated with the pump pulses or obtained from the second harmonic of the Nd:YAG laser ($\hbar\omega_T = 2.33$ eV, $\lambda_T = 532$ nm). In our experiments, we adopt a configuration in which the phase mismatch can be neglected (thin grating configuration). Therefore, the diffraction efficiency η is proportional to

$$\eta = \frac{I_D}{I_T} \propto |\Delta\tilde{n}|^2, \tag{1}$$

where I_D is the intensity of the diffracted beam, I_T the intensity of the test beam, and $\Delta\tilde{n}$ the change of the complex index of refraction. We obtain the temporal variation of the diffraction efficiency by passing the probe pulse through an optical delay line. If the excited quasiparticles decay exponentially with a time constant T_1, the characteristic time of the grating relaxation τ_g as a function of the fringe spacing can be written as[14]

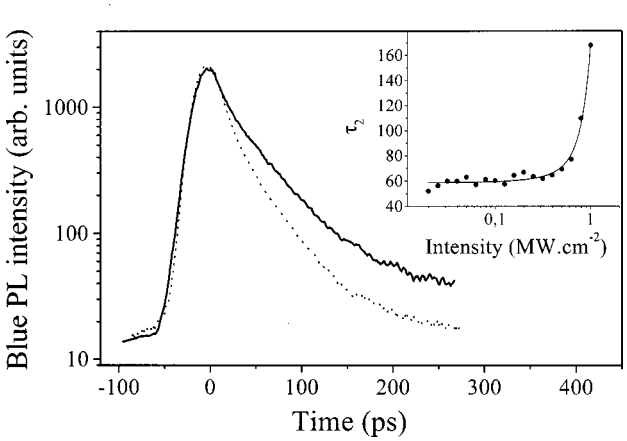

FIG. 2. Dynamics of the blue PL intensity for different excitation intensities (line: 800 kW cm^{-2}, dots: 300 kW cm^{-2}). The inset shows the long-decay time constant of the blue luminescence as function of excitation intensity.

$$\frac{1}{\tau_g} = \frac{1}{T_1} + \frac{4\pi^2 D}{\Lambda^2}, \tag{2}$$

where D is the ambipolar diffusion coefficient. Measuring τ_g for different fringe spacing, T_1 and D can be determined separately.[15]

Temperature-dependence experiments are finally performed by placing the sample into a continuous helium flow cryostat equipped with a temperature controller.

III. DYNAMICS OF CARRIER RELAXATION AT ROOM TEMPERATURE

A. Study of the blue and yellow luminescence

In this section, we compare the dynamics of the blue and the yellow luminescence for different intensities of excitation at room temperature. Let us first discuss the blue luminescence (Fig. 2). Results exhibit two excitation regimes. At low intensities ($I < 500$ kW cm^{-2}), the blue luminescence exhibits a biexponential decay, with characteristic times $\tau_1 = 25$ ps and $\tau_2 = 60$ ps, respectively, which are of the same order of magnitude as that of other works.[16,17] In this low-excitation regime, τ_1 and τ_2 are found to be independent of the excitation intensity, also in agreement with the literature.[18] The temporal behavior of the blue luminescence become different for $I > 500$ kW cm^{-2}. With increasing excitation intensity, the first decay time τ_1 of the blue luminescence remains constant, equal to 25 ps. Then, as shown in the inset of Fig. 2, τ_2 increases drastically, reaching 170 ps for an intensity of 1 MW cm^{-2}. As shown in Fig. 3, the dynamics of the yellow luminescence exhibits the same intensity dependence as the blue luminescence. For low excitations, the yellow luminescence exhibits a single short decay time, which is close to our experimental resolution. After deconvolution with the exciting pulse, it is estimated to be inferior but about 20 ps. This characteristic time, measured for all of our samples, strongly differs with published decay times of the yellow luminescence,[19,20] which are often given on the microsecond scale. This difference may be due to the duration of our exciting pulse (25 ps), the relatively high excitation intensity and to the associated detection system,

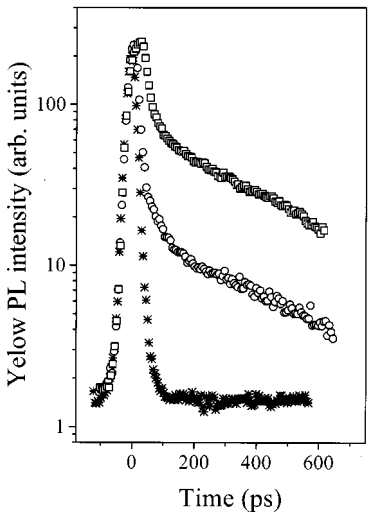

FIG. 3. Dynamics of the yellow luminescence for different excitation intensities. (squares: 750 kW cm^{-2}, circles: 550 kW cm^{-2}, stars: 400 kW cm^{-2}).

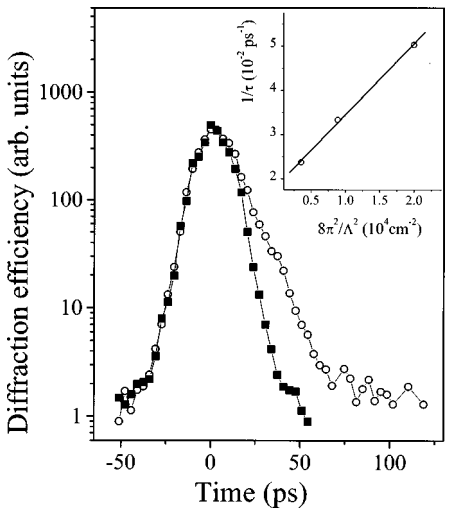

FIG. 4. Dynamics of the diffraction efficiency with (open circles) and without (filled squares) prepulse. Inset: characteristic decay time τ of the grating for different fringe spacings in the presence of a prepulse (open circles) and fit with Eq. (2) (full line).

sensitive on a nanosecond scale. Therefore, this experimental situation is different from that of Ref. 19 (10 ns excitation, luminescence measured with a storage oscilloscope) and from Ref. 20 (3 μs excitation, luminescence measured with a phosphorimeter). In addition, samples of Refs. 19 and 20 are grown by molecular-beam epitaxy with a growth temperature, which generally do not exceed 1100 K. The density of defects of these samples should be larger than those obtained by MOCVD.

When exceeding 500 kW cm^{-2}, the yellow luminescence shows a double exponential decay with time constants of about 25 and 430 ps, which are independent of the excitation intensity. The long-lasting contribution to the yellow luminescence increases with increasing excitation intensity.

In order to complete our luminescence study, we measure the blue luminescence spectra for an excitation intensity of 300 and 800 kW cm^{-2}, which corresponds to the two excitation regimes. It appears that 300 kW cm^{-2} pulses only enlarge the band-gap luminescence due to collision processes, whereas 800 kW cm^{-2} pulses generate hot luminescence. We also measure the intensity of the blue and yellow luminescence as a function of the excitation intensity. We find a linear increase of the blue luminescence intensity and a square-root dependence for the yellow luminescence with increasing pump-beam intensity. This behavior was previously observed by Grieshaber *et al.*[21] in the stationary regime. They interpreted these results by using a set of bimolecular rate equations between shallow impurities, deep levels, and continuum states. Such bimolecular recombination processes, proportional to the probability that thermalized electrons and holes interact, are generally used to explain the formation of excited carriers in GaN samples.[22]

As will be discussed in detail, all these results indicate that, at room temperature, defect states responsible for the yellow and partly to the blue luminescence become saturated under high excitations conditions.

B. Degenerate four-wave mixing experiments using a prepulse

We study in this section four-wave mixing experiments at room temperature, using the third harmonic of the Nd:YAG laser ($\hbar\omega = 3.49$ eV), i.e., when exciting close to the band edge. Degenerate four-wave mixing experiments in a standard three-beam configuration, published in a previous article,[23] have shown that the diffraction efficiency rapidly decreases with a constant characteristic time of about 25 ps. In addition, no diffusion processes have been observed, indicating either that the lifetime of the carriers is too short, or that they are rapidly trapped by deep impurities levels. In order to distinguish between these possibilities, we now use a prepulse arriving 60 ps before the two pump pulses, in order to saturate the trapping states. The intensity of the prepulse is 800 kW cm^{-2} and the intensity of the three other pulses is 150 kW cm^{-2} each. Figure 4 shows the dynamics of the diffraction efficiency with and without prepulse for a fringe spacing of 6.4 μm. It appears that the saturation induced by the prepulse affects the decay time of the diffraction efficiency, which increases from 25 to 50 ps. The measurement of the grating relaxation time for different fringe spacing (inset of Fig. 4) leads to a value of the carrier relaxation time $T_1 = 54$ ps. The ambipolar diffusion coefficient is found to be $D = 0.16$ cm^2/s. This relative small value compared with other semiconductors,[24] is in agreement with electron-beam-induced current experiments,[25] which report a value of 0.12 cm^2/s. This value was tentatively explained by carrier recombination at linear dislocations after diffusion into columnar defect-free domains, which have a typical size of 0.4 μm. In our case, however, the diffusion length L_d is given by

$$L_d = \sqrt{DT_1}, \tag{3}$$

which is found to be about 300 Å. This value is one order of magnitude smaller than the expected size of the columnar domains. On an other hand, electron ballistic transport in GaN has been studied by Monte Carlo simulations.[26] This modelization predicts a diffusion length of about 150 Å due to the strong electron-phonon coupling. This value, which is

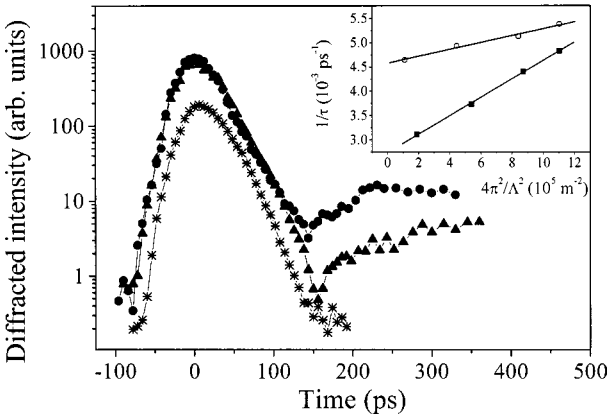

FIG. 5. Dynamics of the diffracted beam for different intensities of excitation (circles: 900 kW cm^{-2}, triangles: 600 kW cm^{-2}, stars: 300 kW cm^{-2}). Inset: grating relaxation time τ for different fringe spacings for an excitation intensity of 300 kW cm^{-2} (circles) and 800 kW cm^{-2} (squares).

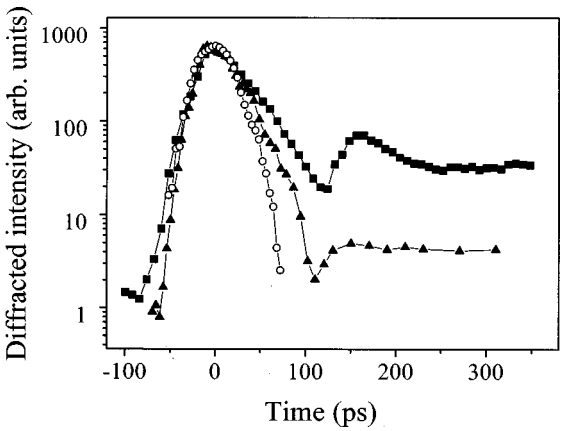

FIG. 6. Diffusion time for different samples, characterized by their ratio r between the intensity of the blue and the yellow luminescence. Squares: $r=0.5$; triangles: $r=50$; circles: $r=400$.

comparable to our results, also shows the strong contribution of nonradiative recombination processes due to electron-phonon scattering.

C. Nondegenerate four-wave mixing experiments

At room temperature, we study the transition between shallow donor and deep acceptor states by nondegenerate four-wave mixing experiments in a three-beam configuration. The probe pulses are obtained from the second harmonic of the Nd:YAG laser at 2.33 eV, which roughly corresponds to the maximum of the yellow-luminescence line of the sample. Pump pulses, generated by the third harmonic of the Nd:YAG laser, excite the sample at 3.49 eV. Therefore, in this configuration, we can test the optical nonlinearity induced by the pump beam but in the spectral region of the transitions between the defect states.

We first determine the intensity dependence of the diffraction efficiency at temporal coincidence. Measurements, performed with a fringe spacing of 7.1 μm, show a saturation of the diffraction efficiency for $I>40$ kW cm^{-2}. As pointed out in Ref. 27, this behavior is attributed to the contribution of higher orders of the nonlinear susceptibility. Consequently, since we are working at high intensity of excitation, our further conclusions will concern rather $|\Delta\tilde{n}|$ than $|\chi^{(3)}|$.

1. Intensity dependence

As in time-resolved luminescence experiments, the dynamics of the diffraction efficiency (Fig. 5) exhibits two excitation regimes: for $I<I_S=500$ kW cm^{-2} the grating relaxes with a characteristic time of about 45 ps, which is found to be independent of the excitation intensity. For $I>I_S$, the dynamics of the diffraction efficiency exhibits a singularity around 150 ps : the signal decreases down to the noise level, then increases again and reaches a constant value. According to Eq. (1), we attribute this behavior to a change of the sign of the real part of the index of refraction change $\Delta\tilde{n}$. This can be due to a competition between a negative contribution due to electronic processes ($\Delta n_{\text{electronic}}<0$ in the Drude model), and a positive contribution due to heating processes ($\Delta n_{\text{thermic}}>0$ due to a shrinkage of the band gap) (Ref. 28)

$$|\Delta\tilde{n}|^2=|\Delta n_{\text{thermic}}+\Delta n_{\text{electronic}}|^2. \tag{4}$$

The thermal process, induced by nonradiative relaxation of trapped carriers in the deep levels to valence-band states, appears about 150 ps after excitation. This is in agreement with the dynamics of the yellow luminescence, which also exhibits the saturation component 150 ps after the exciting pulse, corresponding to the filling time of trapping levels.

This interpretation is confirmed by the measurement of the grating relaxation dynamics for different samples (Fig. 6). The optical quality of each sample is characterized by the ratio r between the integrated blue and yellow luminescences intensities, which varies from $r=0.5$ to $r=400$. It appears that the thermal contribution increases when the quality of the sample decreases. In the same time, the electronic decay time decreases when the quality of the sample increases. The experiment performed on a high-quality sample (without any measurable yellow band) does not exhibit any diffracted signal.

2. Determination of the diffusion coefficient

We measure at room temperature the dynamics of the diffraction efficiency for different fringe spacings of the grating. This experiment is performed on the sample with $r=50$, for two excitation intensities of 300 kW cm^{-2} and of 800 kW cm^{-2}, respectively (inset of Fig. 5). These intensities correspond to the two excitation regimes discussed above. The carrier relaxation times corresponding to the shallow donor-deep acceptor transition is found to be about 4.5 and 75 ps at 300 and 800 kW cm^{-2}, respectively. The value of the diffusion coefficient, which is also intensity dependent increases from 0.08 to 0.12 cm^2/s for intensities of 300 and 800 kW cm^{-2}, respectively. This behavior can either be attributed to an intensity dependence of the diffusion time (due to a nonvalidity of Fick's law under high-excitation conditions[29]), or to different hopping rates between trapped states, induce by the saturation process.

D. Discussion

The decay times τ_{mes} determined in time-resolved luminescence measurements is influenced by radiative and nonradiative processes. Therefore, τ_{mes} can be written as

$$1/\tau_{\mathrm{mes}} = 1/\tau_{\mathrm{R}} + 1/\tau_{\mathrm{NR}}, \tag{5}$$

where τ_{R} and τ_{NR} are the characteristic times of the radiative and the nonradiative processes, respectively. The radiative lifetime τ_R can be estimated by using the inverse of the Einstein coefficient, which describes the spontaneous emission probability. Within the effective mass approximation, τ_{R} is given by[30]

$$\tau_R = \frac{2\pi\varepsilon_0 m^* c^3}{n_B e^2 \omega_{\mathrm{CV}}^2 f_{\mathrm{CV}}}, \tag{6}$$

where f_{CV} is the oscillator strength of the transition ($f_{\mathrm{CV}} < 1$), $m^* = 0.15 m_0$ is the effective mass of free carriers, $n_{\mathrm{B}} = 2.4$ is the index of refraction and $\omega_{\mathrm{CV}} = E_{\mathrm{CV}}/\hbar = 2.10^{15}\,\mathrm{s}^{-1}$ is the frequency associated with the electronic transition between conduction and valence band. For GaN, we obtain a radiative lifetime on the nanosecond scale. Therefore, we can assume that, at low intensities, the observed decay times are dominated by nonradiative processes. This is especially true for the yellow luminescence.

For intensities $I > I_S = 500\,\mathrm{kW\,cm^{-2}}$, all our experiments show a saturation threshold in the blue as well in the yellow spectral region. Owing to the fact that this saturation occurs for the same excitation intensity, we assume that the blue and the yellow luminescence involve one and the same level, i.e., that the yellow luminescence is due to a radiative transition from shallow donor to deep acceptor levels[31] and that the blue luminescence is partly due to the recombination of an exciton bound to the shallow donor (I_2 line). In order to fit the temporal behavior of the luminescence signal, we use a set of bimolecular-rate equations between free, bound, and trapped carriers. We introduce a saturation term of the shallow donors and the deep acceptor centers, in order to explain the high-excitation regime. This model is illustrated in Fig. 7 and the rate equations read

$$\begin{cases} \dfrac{dn_C}{dt} = G(t) - \dfrac{1}{\tau_{\mathrm{CV}}} n_C n_h - \dfrac{1}{\tau_{\mathrm{CD}}} n_C (n_D^0 - n_D) \\ \dfrac{dn_D}{dt} = \dfrac{1}{\tau_{\mathrm{CD}}} n_C (n_D^0 - n_D) - \dfrac{1}{\tau_{\mathrm{DV}}} n_D n_h - \dfrac{1}{\tau_{\mathrm{DT}}} n_D (n_T^0 - n_T) \\ \dfrac{dn_T}{dt} = \dfrac{1}{\tau_{\mathrm{DT}}} n_D (n_T^0 - n_T) - \dfrac{1}{\tau_{\mathrm{TV}}} n_T n_h \\ \dfrac{dn_h}{dt} = G(t) - \dfrac{1}{\tau_{\mathrm{CV}}} n_C n_h - \dfrac{1}{\tau_{\mathrm{DV}}} n_D n_h - \dfrac{1}{\tau_{\mathrm{TV}}} n_T n_h \end{cases}, \tag{7}$$

where n_C, n_D, n_T, and n_h represent the density of free carriers in the conduction band (3.49 eV), occupied donor states (3.44 eV), deep-trap states (1.0 eV), and holes, respectively. τ_{CD} is the relaxation time from the conduction band to the shallow donors levels, τ_{CV} from the conduction to the valence band, τ_{DV} from the donor states to the valence band, τ_{DT} from shallow donor levels to the deep trap states, and τ_{TV} from these trap states to the valence band. n_D^0 and n_T^0 represent the total density of neutral donors and trap levels, respectively. $G(t)$ describes the generation rate, i.e. reproduces the temporal shape of the laser pulses.

When analyzing the luminescence and the different four-wave-mixing experiments in the frame of this model, the following relaxation scenario is obtained: after excitation, hot carriers thermalize to the minimum of the conduction band within a very short time, typically of 0.1 ps. Then, excited carriers can either recombine to the valence band with a decay time of $\tau_{\mathrm{CV}} = 170\,\mathrm{ps}$, or be trapped by shallow donor states with a characteristic time of $\tau_{\mathrm{CD}} = 25\,\mathrm{ps}$. These trapped carriers recombine radiatively to the valence band ($\tau_{\mathrm{DV}} = 70\,\mathrm{ps}$) or to the deep trap states ($\tau_{\mathrm{DT}} = 4.5\,\mathrm{ps}$), generating part of the blue and the yellow luminescence, respectively. The carriers trapped in the deep levels relax nonradiatively with a characteristic time of about 430 ps, giving rise to lattice heating. The origin of this long-decay time is tentatively attributed to bottleneck effects in multiphonon nonradiative relaxation,[32] which give rise to an intensity dependence of the nonradiative decay time. At high-excitation intensities, trap states and neutral donor levels saturate and carriers stay in the conduction band, which lead to the hot blue luminescence. This hot luminescence also explains the difference between decay times of blue and yellow luminescence for the high-intensity regime, which adds a supplementary recombination path.

We stress that, according to Eq. (5), all these observed decay times are related to radiative and nonradiative decay processes. Having the different decay times given above, the best fit of Eq. (7) leads to a concentration of neutral donors and trap states,[33] which are found to be $n_D^0 = 6.10^{17}\,\mathrm{cm^{-3}}$ and $n_T^0 = 2.10^{16}\,\mathrm{cm^{-3}}$ for the sample with $r = 50$. These values do not only fit the temporal behavior of the luminescence signal, but give also the order of magnitude of the ratio between blue and yellow luminescence intensities. The relative high value of n_D^0 is responsible for the large contribution of the I_2 line to the blue luminescence signal, observed for low excitation intensities. On the other hand, the value of n_T^0 is interpreted as the impurity concentration.

We notice that this scenario is in agreement with pump and probe experiments performed under resonant and nonresonant excitation conditions. In Ref. 23, an increase of the lattice temperature was observed under high band-to-band excitation, which is not present under resonant excitation

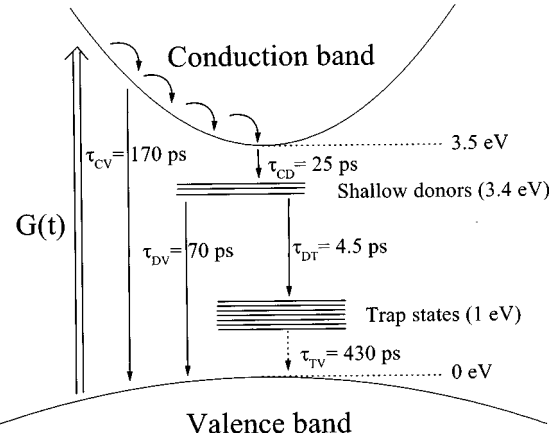

FIG. 7. Scenario of radiative (→) and nonradiative (– – – –>) transitions of GaN under resonant band-to-band excitation (⇒).

conditions. This thermal effect was attributed to the carrier relaxation within the continuum states of the conduction band. At the same time, we find here a strong contribution of the nonradiative processes on the dynamics of carrier relaxation, which leads to a temperature increase also under resonant excitation conditions. This behavior is explained by a rapid capture of carriers, followed by a long-nonradiative relaxation from the deep-trap states.

We also stress that our saturation intensity corresponds to the threshold of stimulated emission of GaN layers, measured at room temperature by several groups.[34,35] If there is still no general picture of the gain mechanisms in GaN, it is generally accepted that the recombination of an electron-hole plasma (EHP) probably governs the gain mechanisms at room temperature.[36,37] Our experiments lead to the conclusion that stimulated emission (and hence gain) appears when the deep levels saturate and an EHP can build up.

IV. TEMPERATURE DEPENDENCE

In order to characterize the nonradiative processes in the GaN samples, the temperature dependence of the dynamics of the excitonic luminescence intensity have been widely studied. When increasing the lattice temperature from 2 to about 200 K, it is generally found that the intensity of the blue luminescence decreases,[38] reflecting the growing importance of nonradiative processes. On an other hand, the decay time of the blue luminescence tends to increase slightly with temperature, due to a thermal detrapping of carriers from the recombination centers.[39] We present in this section the temperature behavior of our sample under high-excitation intensities.

When decreasing the lattice temperature of the sample from 300 K, all our measurements exhibit the same temperature dependence. For $I > I_S$, the slow components of the blue and the yellow luminescence disappear at 200 K. Using nondegenerate four-wave mixing, we study at temporal coincidence the temperature variation of the diffraction efficiency at 2.33 eV. Experiments are performed with an excitation intensity of 800 kW cm^{-2} and a fringe spacing of 7.1 μm. When cooling the sample, the intensity of the diffracted signal rapidly decreases and vanishes around 200 K. Degenerate four-wave mixing experiments exhibit the same behavior.

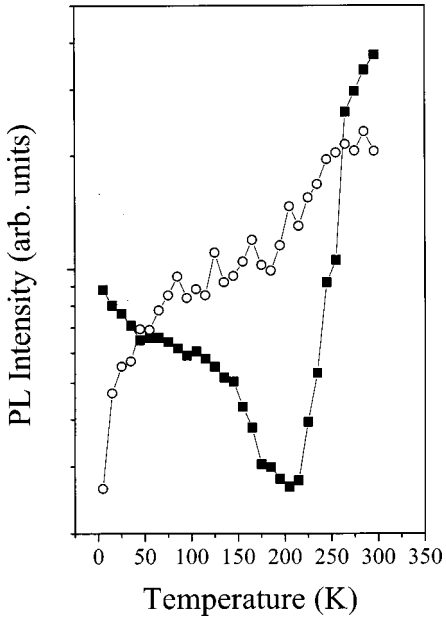

FIG. 8. Intensities of the blue (squares) and yellow (circles) luminescence for different lattice temperatures.

Indeed, no change in the dynamics of the diffraction efficiency is observed by the application of a prepulse at 4 K, indicating that deep-trap states do not saturate. Therefore, we assume that the saturation regime is only observable for temperatures higher than 200 K. In order to determine the origin of this behavior, we measure the temperature dependence of the blue and yellow luminescence intensities for an excitation intensity of 800 kW cm^{-2} (Fig. 8).

When increasing the lattice temperature from 4 to 200 K, the intensity of the blue luminescence decreases whereas the intensity of the yellow luminescence slightly increases. For temperatures higher than 200 K, the intensity of the blue luminescence strongly increases whereas the intensity of the yellow band tends to saturate. This increase of the blue luminescence intensity is due to the hot luminescence which is attributed to the stimulated emission of the EHP.[36]

We tentatively explain these results by the increase of the quasi-Fermi energy with lattice temperature, which fills the deep acceptor states and thus favors their saturation. This model is also in agreement with the results of Ref. 34, where the temperature dependence of the gain threshold of GaN epilayers is studied. This article evidences that exciton-exciton scattering is the dominant gain mechanism at low temperatures, whereas recombination from the EHP is responsible for stimulated emission for temperatures higher than 200 K. Again, a saturation of deep levels quenches the yellow recombination path, which increases the density of carriers in the conduction band and allows the EHP to build up.

V. CONCLUSION

The dynamics of carrier relaxation in gallium nitride has been studied by time-resolved luminescence, degenerate, and nondegenerate four-wave-mixing experiments. Our measurements, performed in the picosecond regime, account for the recombination scenario and lead to a complete set of decay

times between conduction band, shallow donors, deep acceptors, and valence-band states. We also find a saturation of trapped carriers for an excitation intensity of 500 $kW\,cm^{-2}$ due to a saturation of shallow donor and deep acceptor centers. A long-lasting nonradiative decay of the carrier population in the deep trap states is found. This saturation threshold appears at the same excitation intensity as the gain threshold for the electron-hole plasma, indicating that an EHP only can build up when the defect states are occupied. This long-nonradiative decay time of the trapped carriers and the strong increase of the blue luminescence at room temperature reduces nonradiative energy dissipation responsible for optical damage of nitride devices.

ACKNOWLEDGMENTS

The authors are grateful to Dr. C. Guénaud, Dr. P. Gilliot, and Dr. R. Lévy for many helpful discussions and for their critical reading of the manuscript.

[1] P. Rigby, Nature (London) **384**, 610 (1996).
[2] S. Nakamura, T. Mukai, and M. Senoh, Appl. Phys. Lett. **64**, 1687 (1994).
[3] Eunsoon Oh, Hyeongsoo Park, and Yongjo Park, Appl. Phys. Lett. **72**, 1848 (1998).
[4] M. Godlewski, E. M. Goldys, M. R. Phillips, R. Langer, and A. Barski, Appl. Phys. Lett. **73**, 3686 (1998).
[5] E. R. Glaser, T. A. Kennedy, K. Doverspike, L. B. Rowland, D. K. Gaskill, J. A. Freitas, Jr., M. Asif Khan, D. T. Olson, J. N. Kuznia, and D. K. Wickenden, Phys. Rev. B **51**, 13 326 (1995).
[6] P. Perlin, T. Suski, H. Teisseyre, M. Leszczynski, I. Grzegory, J. Jun, S. Porowski, P. Boguslawski, J. Bernholc, J. C. Chervin, A. Polian, and T. D. Moustakas, Phys. Rev. Lett. **75**, 296 (1995).
[7] S. J. Rhee, S. Kim, E. E. Reuter, S. G. Bishop, and R. J. Molnar, Appl. Phys. Lett. **73**, 2636 (1998).
[8] E. Calleja, F. J. Sánchez, D. Basak, M. A. Sánchez-García, E. Muñoz, I. Izpura, F. Calle, J. M. G. Tijero, J. L. Sánchez-Rojas, B. Beamont, P. Lorenzini, and P. Gibart, Phys. Rev. B **55**, 4689 (1997).
[9] D. C. Look, D. C. Reynolds, J. W. Hemsky, J. R. Sizelove, R. L. Jones, and R. J. Molnar, Phys. Rev. Lett. **79**, 2273 (1997).
[10] D. Kim, I. H. Libon, C. Voelkmann, Y. R. Shen, and V. Petrova-Koch, Phys. Rev. B **55**, 4907 (1997).
[11] T. Suski, P. Perlin, H. Teisseyre, M. Leszczynski, I. Grzegory, J. Jun, M. Bockowski, S. Porowski, and T. D. Moustakas, Appl. Phys. Lett. **67**, 2188 (1995).
[12] P. Lefebvre, J. Allègre, B. Gil, A. Kavokine, H. Mathieu, W. Kim, A. Salvador, A. Botchkarev, and H. Morkoç, Phys. Rev. B **57**, 9447 (1998).
[13] H. Haag, S. Petit, P. Gilliot, R. Lévy, O. Briot, and R. L. Aulombard, Mater. Sci. Eng., B **50**, 197 (1997).
[14] J. Eichler, P. Günter, and D. W. Pohl, *Laser Induced Gratings* (Springer, Berlin, 1979), Vol. 50.
[15] P. Riblet, C. Spiegelberg, P. Faller, P. Gilliot, J. Puls, F. Henneberger, and B. Hönerlage, Opt. Mater. **3**, 139 (1994).
[16] G. D. Chen, M. Smith, J. Y. Lin, H. X. Jiang, M. Asif Khan, and C. J. Sun, Appl. Phys. Lett. **67**, 1653 (1995).
[17] W. Shan, X. C. Xie, J. J. Song, and B. Goldenberg, Appl. Phys. Lett. **67**, 2512 (1995).
[18] S. Pau, Z. X. Lin, J. Kuhl, J. Ringling, H. T. Grahn, M. A. Khan, and C. J. Sun, Phys. Rev. B **57**, 7066 (1998).
[19] D. M. Hofmann, D. Kovalev, G. Steude, B. K. Meyer, A. Hoffmann, L. Eckey, R. Heitz, T. Detchprom, H. Amano, and I. Akasaki, Phys. Rev. B **52**, 16 702 (1995).
[20] R. Seitz, C. Gaspar, T. Monteiro, E. Pereira, M. Leroux, B. Beaumont, and P. Gibart, MRS Internet J. Nitride Semicond. Res. **2**, 36 (1997).
[21] W. Grieshaber, E. F. Schubert, I. D. Goepfert, R. F. Karliek, Jr., M. J. Schurmann, and C. Tran, J. Appl. Phys. **80**, 4615 (1996).
[22] S. Pau, J. Kuhl, M. A. Khan, and C. J. Sun, Phys. Rev. B **58**, 12 916 (1998).
[23] H. Haag, P. Gilliot, R. Lévy, B. Hönerlage, O. Briot, S. Ruffenach-Clur, and R. L. Aulombard, Phys. Rev. B **59**, 2254 (1999).
[24] F. A. Majumder, H.-E. Swoboda, K. Kempf, and C. Klingshirn, Phys. Rev. B **32**, 2407 (1985).
[25] Z. Z. Bandic, P. M. Bridger, E. C. Piquette, and T. C. McGill, Appl. Phys. Lett. **72**, 3166 (1998).
[26] N. Mansour, K. W. Kim, N. A. Bannov, and M. A. Littlejohn, J. Appl. Phys. **81**, 2901 (1997).
[27] H. Haag, P. Gilliot, B. Hönerlage, O. Briot, S. Ruffenach-Clur, and R. L. Aulombard, Appl. Phys. Lett. **74**, 1436 (1999).
[28] E. Vanagas, J. Moniatte, M. Mazilu, P. Riblet, B. Hönerlage, S. Juodkazis, F. Paille, J. C. Plenet, J. G. Dumas, M. Petrauskas, and J. Vaitkus, J. Appl. Phys. **81**, 3586 (1997).
[29] B. Hönerlage, Opt. Mater. **1**, 133 (1992); J. Lumin. **54**, 113 (1992).
[30] D. L. Dexter, in *Solid State Physics*, edited by F. Seitz and D. Turnbull (Academic, New York, 1958), Vol. 6.
[31] R. Klann, O. Brandt, H. Yang, H. T. Grahn, and K. H. Ploog, Appl. Phys. Lett. **70**, 1808 (1997).
[32] F. Auzel and F. Pellé, Phys. Rev. B **55**, 11 006 (1997).
[33] M. Lomascolo, M. Di Dio, D. Greco, L. Calcagnile, R. Cingolani, L. Vanzetti, L. Sorba, and A. Franciosi, Appl. Phys. Lett. **69**, 1145 (1996).
[34] S. Bidnyk, T. J. Schmidt, B. D. Little, and J. J. Song, Appl. Phys. Lett. **74**, 1 (1999).
[35] W. Shan, T. Schmidt, X. H. Yang, J. J. Song, and B. Goldenberg, J. Appl. Phys. **79**, 3691 (1996).
[36] H. Amano and I. Akasaki (unpublished).
[37] J. Holst, L. Eckey, A. Hoffmann, I. Broser, B. Schöttker, D. J. As, D. Schikora, and K. Lischka, Appl. Phys. Lett. **72**, 1439 (1998).
[38] D. A. Turnbull, X. Li, S. Q. Gu, E. E. Reuter, J. J. Coleman, and S. G. Bishop, J. Appl. Phys. **80**, 4609 (1996).
[39] J. S. Im, A. Moritz, F. Steuber, V. Härle, F. Scholz, and A. Hangleiter, Appl. Phys. Lett. **70**, 631 (1997).